

# NIR-triggered drug release from switchable rotaxane-functionalized silica-covered Au nanorods†

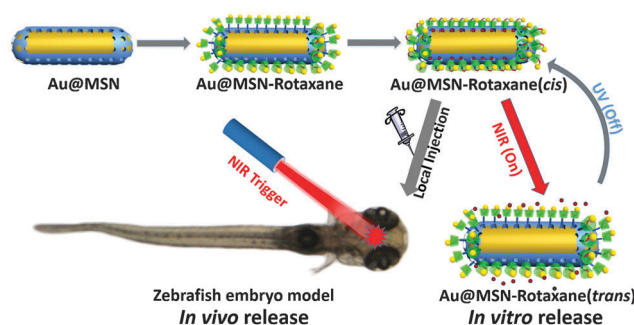
Menghuan Li,<sup>ab</sup> Hong Yan,<sup>a</sup> Cathleen Teh,<sup>c</sup> Vladimir Korzh<sup>c</sup> and Yanli Zhao<sup>\*ab</sup>Cite this: *Chem. Commun.*, 2014, 50, 9745Received 22nd April 2014,  
Accepted 17th June 2014

DOI: 10.1039/c4cc02966f

www.rsc.org/chemcomm

An NIR-triggered drug delivery system was developed by capping photo-switchable azobenzene-based rotaxane onto Au nanorod-mesoporous silica core-shell hybrids. Drug release from the nano-carrier in zebrafish embryo models could be controlled remotely under NIR irradiation, showing significant drug spreading to the adjacent tissues.

Light stimuli, as a remotely-controllable approach, can easily be exerted with high precision and malleability at specific locations.<sup>1</sup> Light-responsive drug delivery systems have received much attention on account of their capability to enhance the drug delivery efficiency and minimize the side effects. Recently, several light-responsive drug carriers based on conformational changes or cleavage of chemical bonds under specific illumination conditions have been reported, including the photoisomerization of azobenzene derivatives,<sup>2</sup> self-assembly and disassembly of pseudorotaxanes,<sup>3,4</sup> and photo-cleavable linkages.<sup>5</sup> For instance, the photoisomerization of azobenzene between the *trans* and *cis* geometries has been utilized to achieve the controlled release of cargo molecules.<sup>6,7</sup> Currently, the majority of these systems have employed UV or visible light as the trigger. However, considering the “water window” (from 700 nm to 1400 nm) of biological tissues for electromagnetic radiation, the tissue penetration of UV and visible light is greatly limited, resulting in inefficient deep-tissue drug delivery.<sup>8</sup> To overcome this challenge, NIR-responsive drug delivery systems are desired. NIR illumination possesses high transmittance and attenuated cytotoxicity in living tissues, and has already been proven as an efficient technique for noninvasive cancer therapy.<sup>9</sup>



**Scheme 1** Illustration of photo-responsive Au@MSN-rotaxane, where the switch of the rotaxane can be controlled remotely by NIR illumination to regulate the cargo release.

Herein, we report the development of an NIR-responsive drug delivery system made by immobilizing azobenzene-based rotaxane onto a Au nanorod-mesoporous silica core-shell hybrid (Au@MSN-rotaxane, Scheme 1 and Scheme S1 in the ESI†). In this system, Au nanorods, a well-proven photothermal agent,<sup>10</sup> serve as the energy converter to activate the isomerization of the azobenzene moiety. The intermediate mesoporous silica layer on the surface of the Au nanorods was used as the drug storage reservoir<sup>11,12</sup> and also as the substrate for post-modification by the rotaxane.<sup>13,14</sup> The rotaxane<sup>15</sup> on the silica layer consists of  $\alpha$ -cyclodextrin ( $\alpha$ -CD) encapsulating the *trans*-azobenzene site, and acts as the capping agent to control the drug loading and release.<sup>16</sup> Initially, the nanocarrier was loaded with cargo molecules *via* diffusion at 40 °C. The cargo-loaded nanocarrier was subsequently illuminated with UV light for robust encapsulation. The cargo release from the nanocarrier was ultimately realized under NIR illumination (Scheme S2 in the ESI†). The delivery efficacy of the nanocarrier was thoroughly investigated in solution and *in vivo* in live zebrafish embryo models.

The Au@MSN-rotaxane nanocarrier was firstly prepared (see ESI† for the experimental procedure) and its physical/chemical properties were characterized in detail. As shown in Fig. 1a, the TEM observations confirmed that the Au nanorods have a uniform and well-defined structure, and this feature was

<sup>a</sup> Division of Chemistry and Biological Chemistry, School of Physical and Mathematical Sciences, Nanyang Technological University, 21 Nanyang Link, Singapore 637371, Singapore. E-mail: zhaoyanli@ntu.edu.sg

<sup>b</sup> School of Materials Science and Engineering, Nanyang Technological University, Singapore 639798, Singapore

<sup>c</sup> Laboratory of Fish Development Biology, Institute of Molecular and Cell Biology, 61 Biopolis Drive, Singapore 138673, Singapore

† Electronic supplementary information (ESI) available: Additional experimental details. See DOI: 10.1039/c4cc02966f

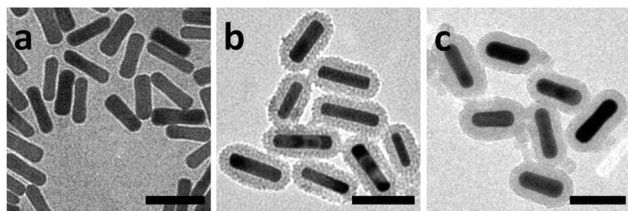


Fig. 1 Illustration of the morphological evolution. TEM images of (a) Au nanorods, (b) Au@MSN, and (c) Au@MSN-rotaxane. Scale bar: 100 nm.

well maintained in the Au@MSN core-shell hybrid (Fig. 1b) and Au@MSN-rotaxane (Fig. 1c). The length and width of the naked Au nanorods were  $75 \pm 15$  nm and  $18 \pm 5$  nm, respectively. The thickness of the mesoporous silica layer coated using the template method was around 10–20 nm. In comparison to the unmodified Au@MSN, Au@MSN-rotaxane appeared to be blurry, which might be due to the modification of the rotaxane on the silica surface.

UV-vis spectra were employed to further characterize the specific electromagnetic absorption of the nanocarrier. As shown in Fig. S2a (ESI<sup>†</sup>), the longitudinal absorption of the naked Au nanorods was centered at 808 nm. After coating with mesoporous silica, it was slightly red-shifted to around 830 nm. This phenomenon could be explained by the Lippert-Mataga equation,<sup>17</sup> as increasing the refractive index of the particle surface from monocrystalline Au substrate (0.28)<sup>18</sup> to silica (1.54)<sup>19</sup> would enhance the localized refraction of the incident light. After the subsequent grafting of the alkyne groups onto Au@MSN, the longitudinal absorption band shifted back to a shorter wavelength of 780 nm. It shifted again to a longer wavelength of 830 nm after the surface immobilization of the photo-switchable rotaxane. In addition, a new peak at 380 nm was observed, which was assigned to the characteristic UV absorption of the azobenzene unit in its *trans* conformation (Fig. S2 in the ESI<sup>†</sup>).<sup>20</sup>

The surface modification process was also monitored by FTIR spectra. As seen from Fig. 2, the coating of mesoporous silica onto the Au nanorods led to a strong peak at around  $1100\text{ cm}^{-1}$ , which was assigned to the Si–O bonds from the silica layer. After the alkyne grafting, a series of new characteristic peaks appeared at 1536, 2100 and 2860, as well as  $2930\text{ cm}^{-1}$ ,

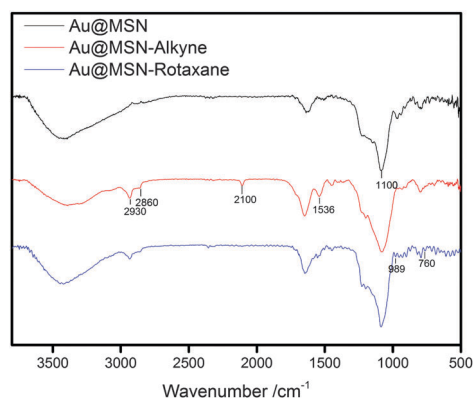


Fig. 2 FTIR spectra of Au@MSN before and after modification. (1) Au@MSN, (2) Au@MSN-alkyne, (3) Au@MSN-rotaxane.

which could be assigned to the amide bond, alkyne end group, and alkyl stretching, respectively. The alkyne-containing Au@MSN subsequently reacted with azidized  $\beta$ -CD-azobenzene pseudorotaxane through a click reaction between the alkyne and azide groups, resulting in the consumption of the alkyne groups. Therefore, the characteristic alkyne peak at  $2100\text{ cm}^{-1}$  disappeared, while some new peaks appeared at 760 and  $989\text{ cm}^{-1}$ , which were assigned to the benzene ring and the sulfonic group<sup>21</sup> on the azobenzene moiety, respectively. The newly appeared peaks indicate that the  $\alpha$ -CD-azobenzene rotaxane was successfully conjugated onto the surface of Au@MSN through the click reaction.

The conformational transition of the azobenzene-based rotaxane in Au@MSN-rotaxane was monitored by UV-vis spectroscopy. It has been reported that UV irradiation can induce the *trans*-to-*cis* photoisomerization of the azobenzene moiety, and that the *cis*-azobenzene can undergo a thermal relaxation process to change back to the *trans* state.<sup>22</sup> The  $\alpha$ -CD ring can effectively encapsulate *trans*-azobenzene but not *cis*-azobenzene, thus leading to UV/heat-controlled  $\alpha$ -CD movement in the rotaxane. When Au@MSN-rotaxane was irradiated with UV light, the absorption at 380 nm decreased due to the *trans*-to-*cis* photoisomerization of the azobenzene unit. Under NIR illumination, a recovery of the absorption intensity in the same region was observed (Fig. 3a), indicating that the *cis*-azobenzene moiety was transformed back to its *trans* state. The absorption intensity change was further plotted against the “on-off” cycle number (Fig. 3b). It was evident that the reversibility between the two isomerization states was well maintained even after 5 cycles. These observations prove that NIR irradiation could efficiently trigger the *cis*-to-*trans* isomerization of the azobenzene moiety for controlled drug release.

Next, a cargo release test from fluorescein isothiocyanate (FITC)-loaded Au@MSN-rotaxane was carried out, and the release profiles were monitored using fluorescence spectroscopy (Fig. 4). In the control group, where the temperature was  $25\text{ }^{\circ}\text{C}$ , it was observed that the amount of FITC released from the FITC-loaded Au@MSN-rotaxane was almost negligible (less than 5%) even after 180 min. In another experiment, when the temperature was increased to  $37\text{ }^{\circ}\text{C}$ , the total release amount of FITC was less than 20%, indicating that the encapsulated cargo molecules could be maintained by the rotaxane cap when no external trigger was exerted. The release profiles in the control experiments matched well with the kinetic features reported in a previous study.<sup>23</sup> In the external heat-triggered

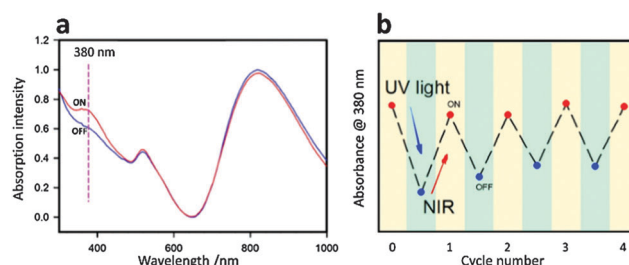


Fig. 3 (a) UV-vis spectra of Au@MSN-rotaxane after treatment with UV irradiation at 365 nm (“on” state) and NIR illumination at 808 nm (“off” state). (b) The changes in the UV absorbance of Au@MSN-rotaxane at 380 nm upon alternating irradiations with UV light and an NIR laser.

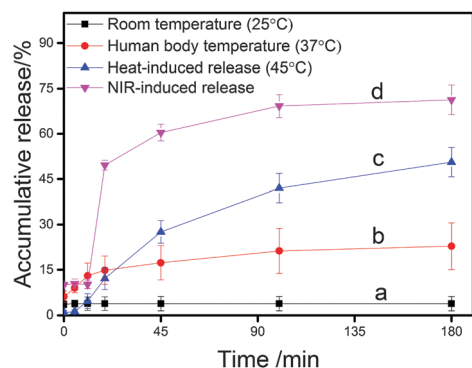


Fig. 4 Release profiles of FITC-loaded Au@MSN-rotaxane in aqueous solution (a) at 25 °C, (b) at 37 °C, (c) with external heating at 45 °C, and (d) under NIR illumination at 808 nm.

group, only a minor increase in FITC fluorescence was observed in the initial 5 min, when the temperature was at 25 °C. Interestingly, the release amount rose rapidly when the incubation temperature increased to 45 °C, and it ultimately reached around 50% in 180 min, which could be explained as the *cis-to-trans* relaxation rate of the azobenzene moiety would speed up under high temperature. When an NIR laser was applied, the loaded FITC was released rapidly into the medium, and the release amount eventually reached approximately 70%. For the NIR-triggered release, there was a delay of approximate 5 min between the launching of NIR illumination and the rapid increase of the fluorescence intensity. The possible reason is that during the photothermal treatment, the Au nanorods may need to first heat up the whole surrounding environment to evoke the relaxation of *cis*-azobenzene on the silica surface, thus causing the delayed drug release in comparison to the external heating method. Overall, the release profiles demonstrated well that this drug delivery system could readily respond to remote NIR irradiation for controlled cargo release.

The *in vivo* release efficiency of Au@MSN-rotaxane loaded with the anticancer drug doxorubicin (DOX)<sup>24</sup> was evaluated in zebrafish embryo models using confocal laser microscopy (CLSM). The confocal images presented a visual demonstration of the distribution of

DOX released from Au@MSN-rotaxane, as DOX itself has strong red fluorescence that facilitates CLSM detection. As compared to the unilluminated control groups, the NIR-illuminated specimens showed greater DOX release. The DOX fluorescence covered a significantly larger area after NIR irradiation (Fig. 5). Moreover, the integrated DOX fluorescence intensity ratio of the NIR illuminated embryo to the control group was 3 : 1. It is important to note that the area injected with DOX-loaded Au@MSN-rotaxane was extracted from the integration area to avoid the interference of unreleased DOX. The difference in the fluorescence intensity suggested that Au@MSN-rotaxane could retain the loaded DOX when no external stimulus was exerted, and was capable of efficiently releasing the DOX cargo under NIR illumination. The drug-release behavior of Au@MSN-rotaxane was further investigated by changing the NIR illumination duration. For those zebrafish embryos treated with NIR light for 10 min, the distance of DOX fluorescence spreading was evidently higher than that of the unilluminated control (Fig. S4a and b in the ESI†). The distance increase indicated that more of the DOX inside the Au@MSN-rotaxane was released into the adjacent tissues under NIR irradiation for 10 min. When the NIR illumination duration was reduced to 5 min, the DOX fluorescence band still overlapped completely with the optically opaque Au@MSN-rotaxane in the merged image (Fig. S4c and d, ESI†). The coincidence indicated that most of the loaded DOX was still entrapped within the nanocarrier at this stage, similar to the unilluminated embryo control. It was also consistent with the kinetic features of the above release profile, where the nanocarrier showed a release delay following NIR irradiation (Fig. 4d). Additional *in vivo* experiments carried out at 37 °C also showed a similar trend, where the maximum duration of NIR illumination was extended to 30 min (Fig. S5, ESI†). The observations firmly supported the hypothesis that DOX release could be effectively controlled by remote NIR illumination.

In conclusion, a novel NIR-responsive nanosystem for anticancer drug delivery has been developed through the integration of Au nanorod, mesoporous silica reservoir and azobenzene-based rotaxane. The *cis-to-trans* isomerization of the azobenzene moiety in the rotaxane could be readily initiated upon photothermal heating with an NIR laser, leading to remotely controlled cargo release from the mesoporous silica reservoir. The drug delivery efficacy of the nanosystem has been demonstrated in solution and in live zebrafish embryo models under NIR laser stimulation. The current research presents a successful example of NIR-controlled drug release *in vivo*.

This research is supported by the National Research Foundation (NRF), Prime Minister's Office, Singapore under its NRF Fellowship (NRF2009NRF-RF001-015) and the Campus for Research Excellence and Technological Enterprise (CREATE) programme-Singapore Peking University Research Centre for a Sustainable Low-Carbon Future, and the NTU-A\*Star Centre of Excellence for Silicon Technologies (A\*Star SERC No.: 112 351 0003).

## Notes and references

- 1 S. Mura, J. Nicolas and P. Couvreur, *Nat. Mater.*, 2013, **12**, 991.
- 2 A. A. Beharry and G. A. Woolley, *Chem. Soc. Rev.*, 2011, **40**, 4422.
- 3 J. Li and X. J. Loh, *Adv. Drug Delivery Rev.*, 2008, **60**, 1000.

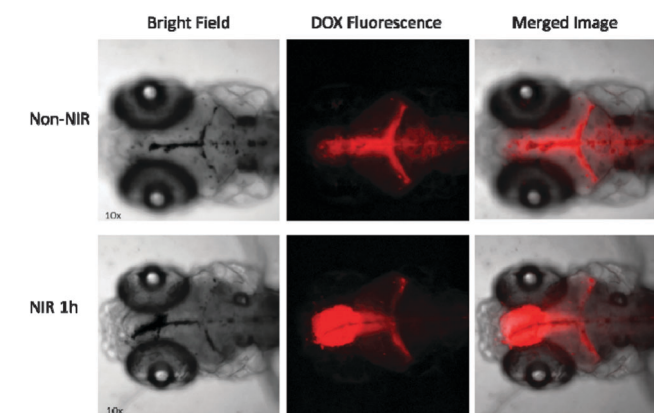


Fig. 5 Confocal images showing the DOX release within embryo heads injected with DOX-loaded Au@MSN-rotaxane without and with NIR irradiation.

- 4 L. Du, S. Liao, H. A. Khatib, J. F. Stoddart and J. I. Zink, *J. Am. Chem. Soc.*, 2009, **131**, 15136.
- 5 N. Z. Knezevic and V. S. Y. Lin, *Nanoscale*, 2013, **5**, 1544.
- 6 J. Liu, W. Bu, L. Pan and J. Shi, *Angew. Chem., Int. Ed.*, 2013, **52**, 4375.
- 7 E. Aznar, M. D. Marcos, R. Martínez-Mañez, F. Sancenón, J. Soto, P. Amorós and C. Guillem, *J. Am. Chem. Soc.*, 2009, **131**, 6833.
- 8 J. Croissant and J. I. Zink, *J. Am. Chem. Soc.*, 2012, **134**, 7628.
- 9 J. V. Frangioni, *Curr. Opin. Chem. Biol.*, 2003, **7**, 626.
- 10 E. C. Dreaden, A. M. Alkilany, X. Huang, C. J. Murphy and M. A. El-Sayed, *Chem. Soc. Rev.*, 2012, **41**, 2740.
- 11 Z. Luo, K. Cai, Y. Hu, L. Zhao, P. Liu, L. Duan and W. Yang, *Angew. Chem., Int. Ed.*, 2011, **50**, 640.
- 12 Q. Zhang, F. Liu, K. T. Nguyen, X. Ma, X. Wang, B. Xing and Y. Zhao, *Adv. Funct. Mater.*, 2012, **22**, 5144.
- 13 M. W. Ambrogio, C. R. Thomas, Y.-L. Zhao, J. I. Zink and J. F. Stoddart, *Acc. Chem. Res.*, 2011, **44**, 903.
- 14 Z. Luo, X. Ding, Y. Hu, S. Wu, Y. Xiang, Y. Zeng, B. Zhang, H. Yan, H. Zhang, L. Zhu, J. Liu, J. Li, K. Cai and Y. Zhao, *ACS Nano*, 2013, **7**, 10271.
- 15 H. Yan, C. Teh, S. Sreejith, L. Zhu, A. Kwok, W. Fang, X. Ma, K. T. Nguyen, V. Korzh and Y. Zhao, *Angew. Chem., Int. Ed.*, 2012, **51**, 8373.
- 16 K. Cai, J. Li, Z. Luo, Y. Hu, Y. Hou and X. Ding, *Chem. Commun.*, 2011, **47**, 7719.
- 17 D. Patra, A. J. Amali and R. K. Rana, *J. Mater. Chem.*, 2009, **19**, 4017.
- 18 P. B. Johnson and R. W. Christy, *Phys. Rev. B: Condens. Matter Mater. Phys.*, 1972, **6**, 4370.
- 19 G. Ghosh, *Opt. Commun.*, 1999, **163**, 95.
- 20 S. Wagner, F. Leyssner, C. Kordel, S. Zarwell, R. Schmidt, M. Weinelt, K. Ruck-Braun, M. Wolf and P. Tegeder, *Phys. Chem. Chem. Phys.*, 2009, **11**, 6242.
- 21 J. Yu, B. Yi, D. Xing, F. Liu, Z. Shao, Y. Fu and H. Zhang, *Phys. Chem. Chem. Phys.*, 2003, **5**, 611.
- 22 H. M. D. Bandara and S. C. Burdette, *Chem. Soc. Rev.*, 2012, **41**, 1809.
- 23 D. Patra and F. Sleem, *Anal. Chim. Acta*, 2013, **795**, 60.
- 24 O. Tacar, P. Sriamornsak and C. R. Dass, *J. Pharm. Pharmacol.*, 2013, **65**, 157.